

MULTIPOLES AND SURMACS II: ENGINEERING

F.F. Chen

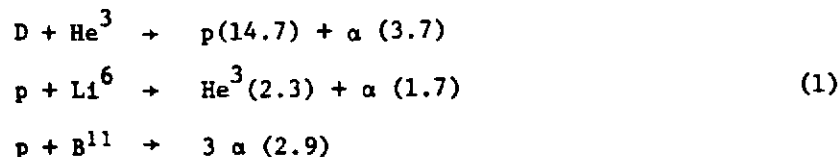
Electrical Sciences and Engineering Department
University of California
Los Angeles, California 90024, USA

INTRODUCTION

Though the engineering of multipoles is in many ways simpler than for toruses with strong toroidal and poloidal fields, the feasibility of multiple floating rings in a reactor environment is of great concern, since it has never been demonstrated even in theory. Recent work by the group at TRW, Inc. and the groups led by R. W. Conn at Wisconsin and UCLA has greatly expanded our data base on the engineering aspects of multipoles. These studies are by no means commensurate with the studies of the physics problems, which have a long history. Nonetheless, there is much more known than can be covered here. The brevity of Part II is due partly to the nature of the calculational results, which are hard to condense, and partly to the necessity to design for specific devices, a process whose results may not be of general or timeless value. A summary of these results already exists¹.

ADVANCED FUEL CYCLES

To evaluate fusion fuel cycles from D-D to p-B¹¹, accurate measurements of many cross sections are needed. The most complete compilation to date was made by a panel of experts assembled by TRW, Inc. and EPRI². For multipole-surmacs these primary reactions producing few neutrons are of greatest interest:



The particle energies are indicated in MeV. Latest cross sections are shown in Fig. 1. Initial optimism on the p-Li⁶ reaction was based on a possible chain reaction involving the energetic He³ product³. However, the reaction He³ + Li⁶ + D + Be⁷ leads to many subsequent events producing neutrons, and a detailed investigation of p-Li⁶ would involve a very complex calculation requiring cross sections that are not well known. Current interest has centered on the "lean" D-He³ reaction, suitable for a low-neutron satellite reactor, and the p-B¹¹ reaction, which has been revived by the calculations of Shuy and Conn⁴.

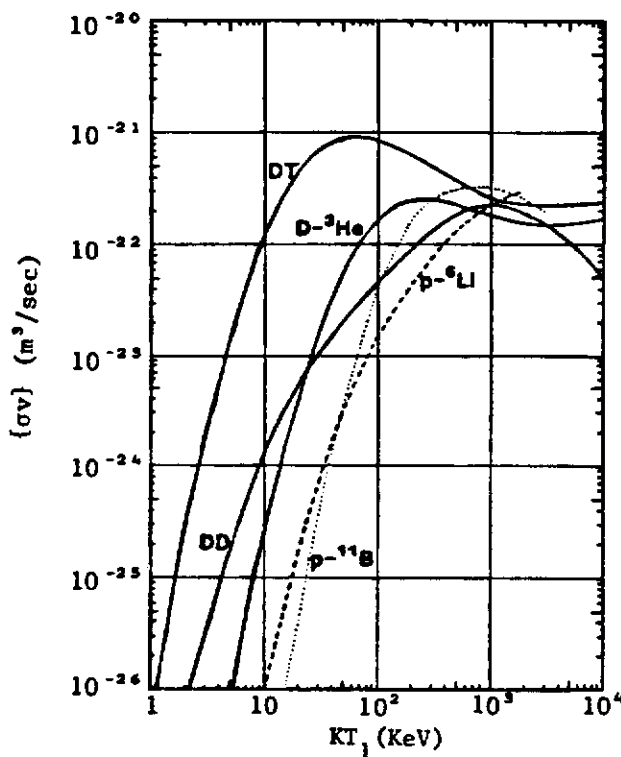


Fig. 1. Advanced fuel reactivities compared to DT.

These authors have calculated the improvement in reactivity due to the interaction of reaction products with the thermal fuel for the D-D, D-He³, and p-B¹¹ cycles. There are four physical processes that are usually neglected when the ash particles are considered to be gradually slowed down by small-angle collisions with the thermal distributions of electrons and fuel ions.

1) Nuclear elastic and inelastic scattering becomes important

relative to Coulomb interactions at typical ash energies of 10 MeV and typical fuel temperatures of 100 keV. Knock-on events produce a high energy tail in the fuel distribution which greatly enhances the probability of fusion. 2) Large-angle Coulomb collisions also populate the ion tail. 3) Thermalization of the tail particles among themselves helps by bringing the superfast particles down to energies near the peak of the fusion cross section. 4) Propagation of high-probability fusion reactions occurs as the processes above keep a high-energy tail populated. An example of a reaction propagation sequence is



where the bar indicates a hyperthermal particle. These do not have to be very abundant to affect the fusion rate because of the steepness of the curves in Fig. 1.

In the computations of Shuy^{4,5}, the ion distribution is divided into a Maxwellian body plus a tail. The body is treated as a continuum, subject to small-angle collisions isolated by adjusting the cutoff parameter in the Coulomb logarithm Λ and to Coulomb-nuclear interference treated by a weighting factor. The tail is subjected to the high energy transfer events by a multi-group technique. Bremsstrahlung and ash removal are considered the only energy sinks. Since $T_e \geq 100$ keV is normal here, bremsstrahlung and electron-ion thermalization are treated relativistically.

The results are extremely encouraging. Fig. 2 shows the reactivity enhancement⁴ due to processes (1)-(4) for the p-B¹¹ reaction, whose main branch is a decay into an α and a Be⁸ nucleus in an excited state, which subsequently decays into two α 's. The enhancement is sensitive to T_e because of the Coulomb drag. When these data are used to compute Q , the values in Table I, showing the possibility of ignition, are obtained^{4,1}. Here Q is the ratio of fusion power to heating power, M the ratio of fusion power to bremsstrahlung and ash removal loss power, and $n\tau_E$ is evaluated for $Q = 5$. The requirements on $n\tau_E$ are about an order of magnitude higher than for DT; furthermore the necessity for large T_e raises problems with synchrotron radiation (see Part I), which has been neglected here. Nonetheless, the results on ion tail promotion encourages further pursuit of the p-B¹¹ cycle, which is almost neutron free. The endothermic reaction $p + B^{11} \rightarrow n + C^{11}$ has a branching ratio $\approx 10^{-3}$.

Similar calculations⁴ for the D-He³ cycle yield the Lawson

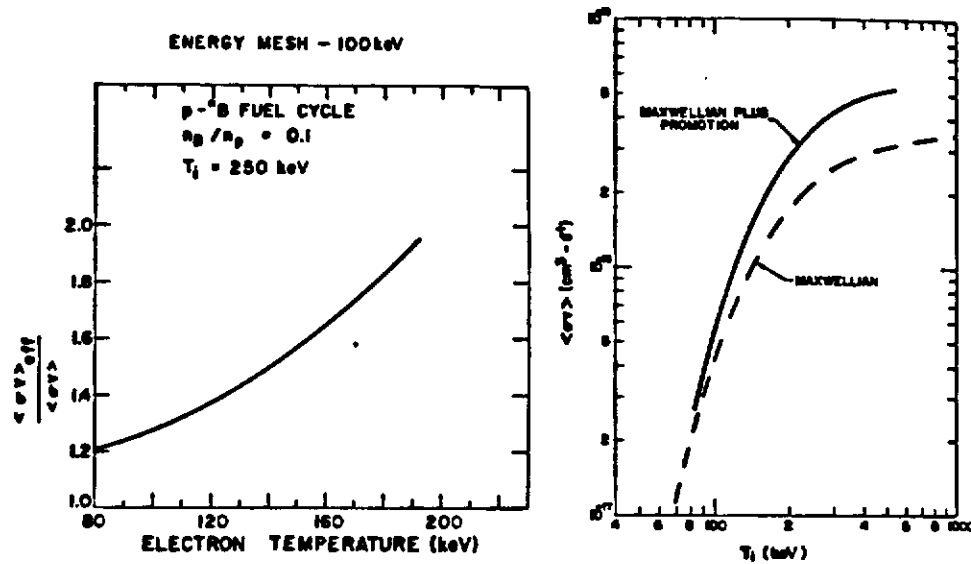


Fig. 2. Reactivity enhancement factor vs. T_e at $T_i = 250$ keV, and reactivity vs. T_i at $T_e = 160$ keV.

Table I. Requirements for a p-B¹¹ Reactor⁴.

T_i (keV)	T_e (keV)	M	Q	$n\tau_E$ (sec/cm ³)
200	140	0.8	4	--
250	155	0.97	32	2.4×10^{15}
300	160	1.08	∞	1.36×10^{15}

curves shown in Fig. 3a. Here the effects of tail promotion lowers the ignition $n\tau_E$ to 3×10^{14} sec/cm³ at $T_i = 100$ keV, the same as for DT at 20 keV. For multipoles, there is then the problem of shielding against the neutrons. Fig. 3b shows the effect on neutron heat load and fusion power of increasing the density ratio of He³ to D. Neutron production can be greatly reduced, but only at the expense of fusion power. For ratios greater than 8, ignition cannot be achieved with D-He³.

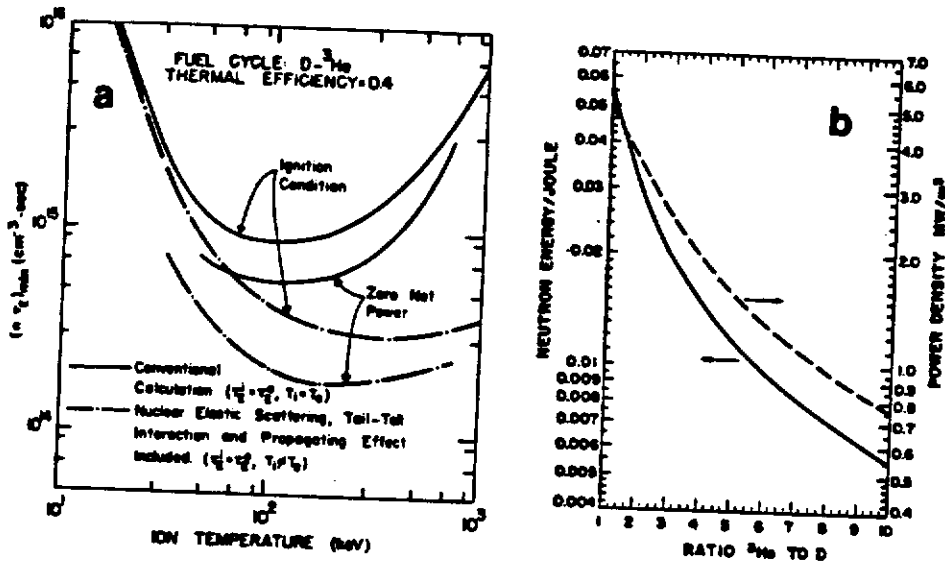


Fig. 3. (a) Improvement of Lawson condition for D-He³ with ion tail formation. (b) Effect on neutron energy and fusion power of running a lean mixture of D and He³.

DESIGN OF SUPERCONDUCTING RINGS

The most critical elements in the design of a multipole or surmac reactor are the superconducting levitated rings, which must maintain an internal temperature of $< 10^{\circ} \text{K}$ while immersed in a reacting plasma of $\geq 2 \times 10^9 \text{K}$. The superconductor must be well shielded; the minor diameter of the rings will therefore be of order 1 m or larger. This consideration sets the scale of the entire reactor. There are at least three ways in which the superconductor can be cooled. First, if magnetically shielded leads are possible, one can imagine continuous circulation of liquid He from the outside. Second, since the rings receive more radiation from the side facing the plasma than the side facing the wall, a temperature gradient will develop across the minor diameter; and one can conceive of incorporating a refrigeration system within each ring that will be driven by this temperature difference. The exhaust heat of the internal cryostat will be radiated away from a high-temperature surface to the outside wall. Third, one can simply replace the rings after their warm-up time of a few days with another set that has been cooled in an adjacent chamber. This conservative approach is the one taken in the three designs described here. The feasibility of levitating a single superconducting ring has already been demonstrated in numerous levitron and spherator experiments.

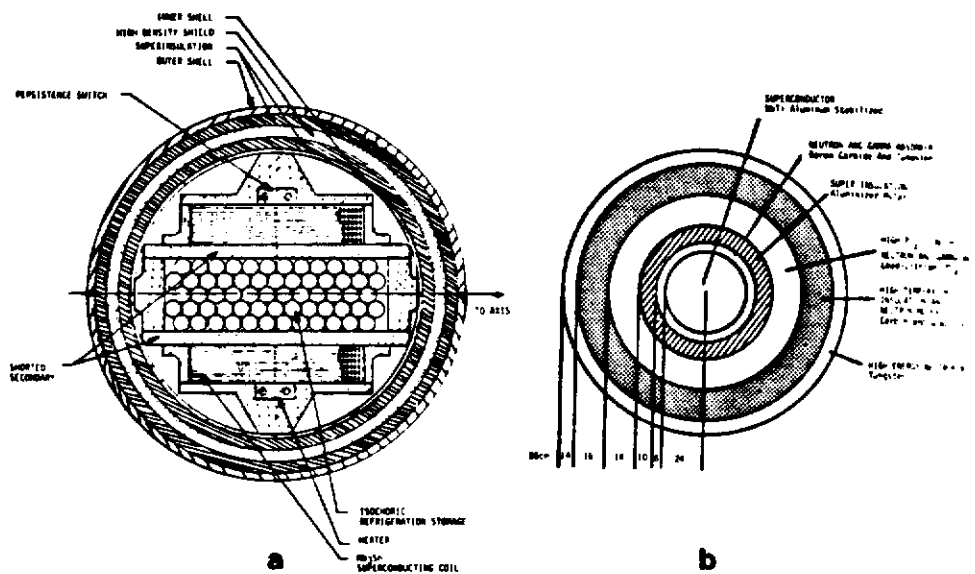


Fig. 4. Superconducting ring designs for (a) a proof-of-principle experiment, and (b) a conceptual D-He³ reactor. (Ref. 2)

The first design, shown in Fig. 4a, is for a proof-of-principle experiment². This ring can remain superconducting for an experimental time of about five hours. Partly to test new technology, it is designed not with NbTi but with multifilament Nb₃Sn wire, which has a critical current density ten times less sensitive to temperature changes at 4.5°K than NbTi. The 4- μ m diam filaments are imbedded in a 2 \times 1 mm matrix, 2200 turns of which carry 909 A each, for a total of 2 MA, 3 to 6 times larger than presently achieved. Protection of the superconductor is by good thermal and electrical contact to thick Al plates, cooled by a reservoir of He providing 1.2×10^4 J of heat capacity between 4.2 and 6.5°K. Peak field is 6.4 T, and stored magnetic energy is 9.6 MJ in the 2 m major by 15.5 cm minor diam. coil.

The second design² (Fig. 4b) is a much larger ring shielded against the neutron and x-ray flux of a conceptual D-He³ reactor. The outside layer is 14 cm of tungsten, which serves both to radiate absorbed x-ray and particle energies at 2000°K and to moderate the neutron spectrum. A layer of high temperature carbon insulation further softens the spectrum. Gamma rays generated in the outer layers are absorbed in a Pb₄Li layer which melts at 507°K and provides thermal capacity. Aluminized mylar superinsulation follows, and a B₄C and W gamma absorber is added inside the superinsulation. The superconductor is NbTi stabilized with Al in a Cu matrix. Construction of the superconductor and dewar is shown in Fig. 5. The coil carries 4.8 kA/cm² at 8 T. The fractional volumes

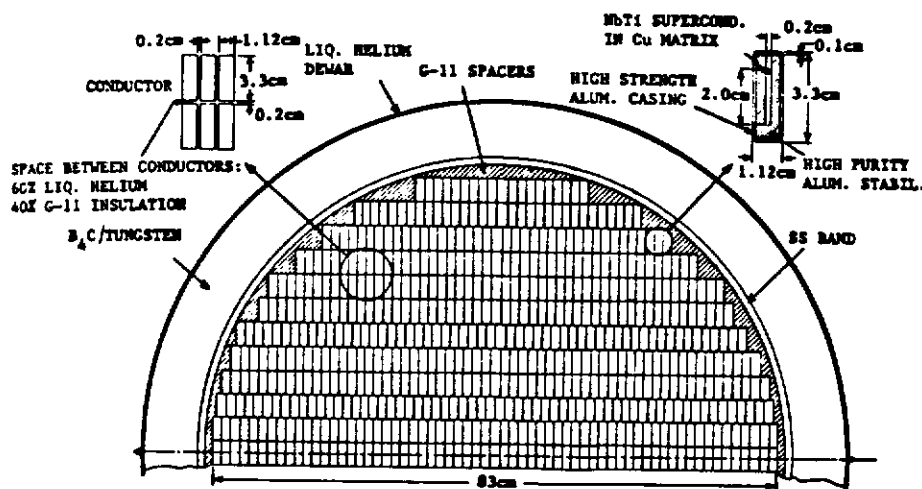


Fig. 5. Superconductor design for conceptual multipole reactor. (Ref. 2)

in the conductor region are: superconductor (18%), Al stabilizer (48%), copper (9%), and liquid He (15%).

Heating of the ring was computed as if it were ≈ 6 m away from a 4.6 m-diam reacting D-He³ plasma. Fig. 6 shows the neutron energy spectrum in such a case; it is dominated by 2.5-MeV D-D and 14-MeV D-T neutrons. The temperature rise in the various layers was then computed under quasi-steady state heating, mainly by the capture of neutrons and of the gamma rays generated thereby. Fig. 7a shows the reduction in neutron flux by the shielding, and Fig. 7b shows the associated volumetric heat source distribution. The ring construction reduces the neutron flux on the axis to $6.3 \times 10^8 \text{ cm}^{-2} \text{ sec}^{-1}$ and the neutron and gamma energy fluxes to 2.5×10^8 and $1.8 \times 10^8 \text{ MeV/cm}^2 \text{ sec}$, respectively. The temperature in the superconductor rises at 0.2°K/hr , allowing operation for the order of a day in this non-optimized design. Neutron damage was also assessed; less than 1% change in resistivity was expected after one year.

The most recent study⁶ of a floating ring design is shown in Fig. 8. The ring is used to provide min- \bar{B} stability in an axisymmetric tandem mirror. The structure of the shielding and insulation is given in Fig. 9. A thermal flux of 45 W/cm^2 is assumed to be incident on the tungsten outer surface in the one dimensional calculation. In addition, the volumetric heating due to neutrons from a D-He³ burn in the geometry of Fig. 8 was included. It is seen from Fig. 9 that the neutron shield in this design holds the temperature of the superconductor below 8°K for the order of five days. With surface heating alone, the time would have been

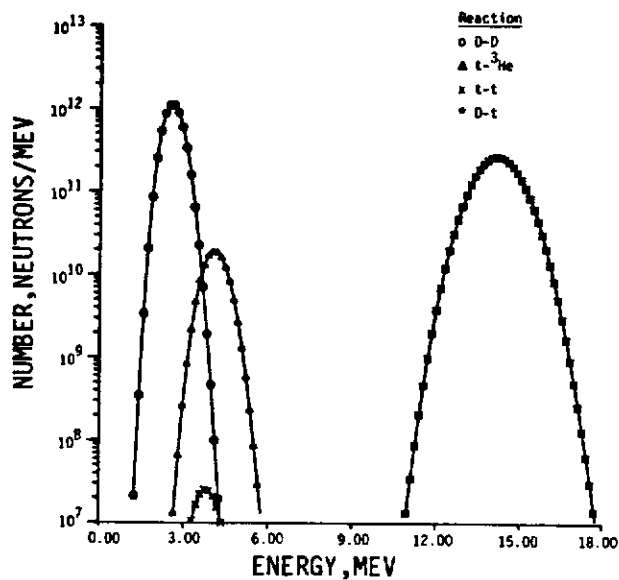


Fig. 6. Neutron energy distribution in a D-He³ reactor. (Ref. 2)

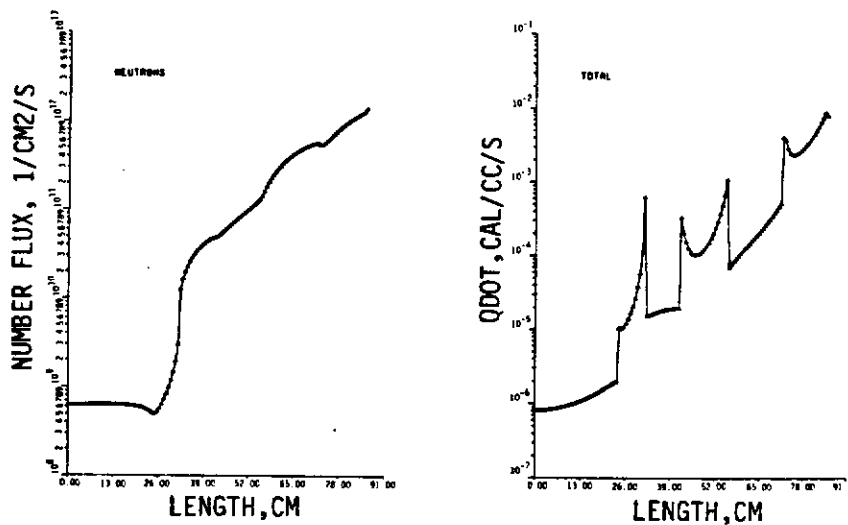


Fig. 7. Neutron flux (a) and volumetric heat source (b) distribution in the ring of Fig. 4. (Ref. 2)

extended to the order of one month. From these computations, it appears that floating rings can be designed for sufficiently long cold times even in the neutron environment of a D-He³ reactor.

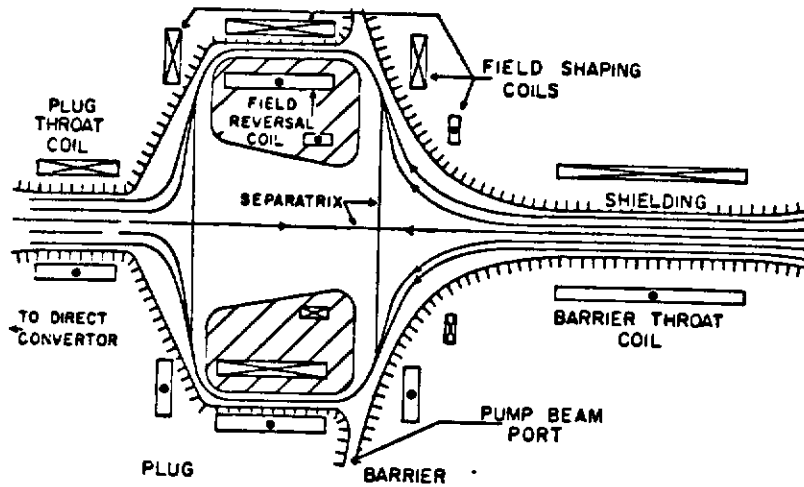


Fig. 8. Geometry of a floating coil designed for an axisymmetric mirror (Ref. 6).

REACTOR DESIGN

We summarize here the main features of a conceptual D-He³ reactor designed by the TRW group². The size and layout of the octupole are shown in Fig. 10, and the numerical parameters in Table II.

In designing the ring sizes, positions, and currents, a compromise has to be made between the engineering constraint of low hoop force and the physics requirement of good wall depth. Furthermore, one has the option of adding an overall bias field to equalize the fields at the bridges of the inner and outer hoops, which tend to differ by about a factor of two. Such a bias field would make better use of the B_{crit} of superconductors and at the same time decrease the mirror ratio and thus tend to suppress trapped-particle instabilities. The present design has a tensile stress on the inner ring and a compressive stress on the outer ring. The upper and lower rings are separated by externally cooled wall hoops carrying about 10 MA. The design is by no means optimized, but it does show that ring stresses and weights can be achieved which are not excessive. The large stored energy is, however, a cause of concern; if one hoop should go normal, some means must be devised to handle the enormous electrical and mechanical loads on a time scale of tens of seconds.

Since most of the fusion power output from an advanced-fuel reactor is in the form of bremsstrahlung x-rays, the heat load on the rings and on the first wall must be considered carefully. The

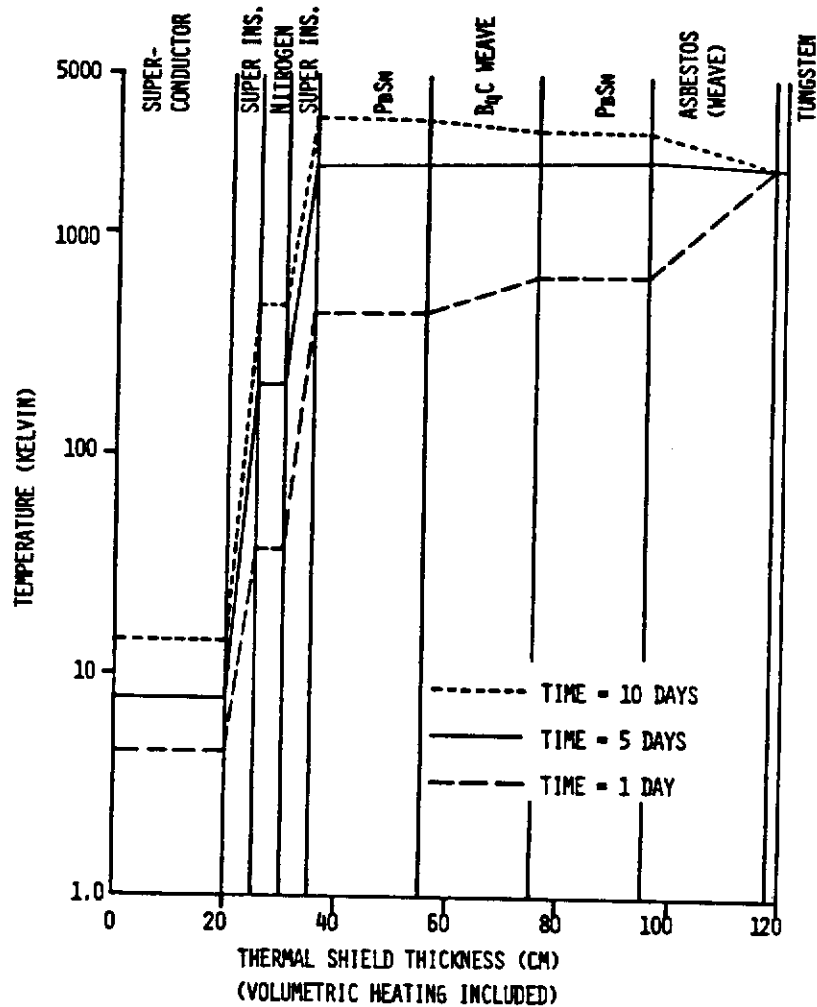
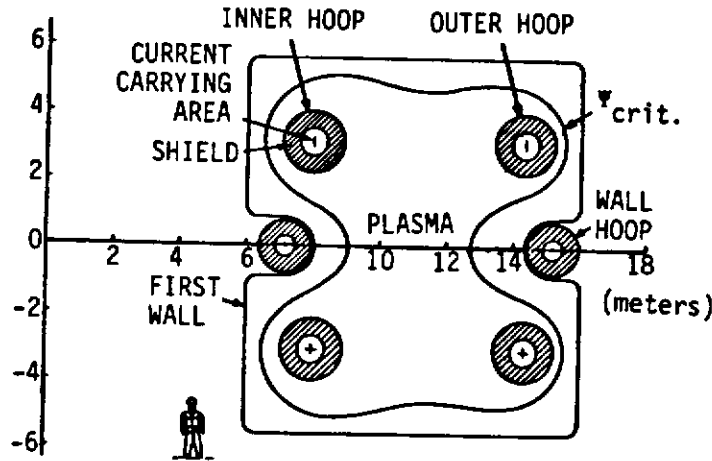


Fig. 9. Temperature distribution in coil of Fig. 8 with volumetric neutron heating (Ref. 6).

floating rings are cooled by radiation from the tungsten surface, limited to a rate of $\approx 1 \text{ MW/m}^2$ at 2000°C . The design of Fig. 10 yields a maximum x-ray flux of 0.69 MW/m^2 on the rings; a further margin of safety can be obtained if the heat is redistributed over the surface by heat pipes. The first wall receives $0.3\text{--}1.11 \text{ MW/m}^2$ x-ray flux, with an average of 0.46 MW/m^2 , well below the wall loading of DT reactor designs. However, the heat load is not well distributed over the volume of the wall. For instance, at $KT_e = 150 \text{ keV}$, 70% of the heat is deposited in the first 0.2 mm of an

80% Va - 20% Ti first wall. The wall material will have to be optimized in regard to mechanical and thermal properties, low-Z contamination, toxicity, and reflectivity for synchrotron radiation; this has not yet been done.



MULTIPOLE FUSION REACTOR

Fig. 10. Schematic of a conceptual D-He³ octupole reactor (Ref. 2).

Table II. Parameters for Conceptual D-He³ Octupole Reactor

Major radius	10.8 m	Ring current (each)	17 MA
Plasma volume	4120 m ³	Power density	0.34 W/cm ³
B _{max} on conductor	9.0 T	Power output	1400 MW _{th}
B at ψ_c	3.7 T	Gross elec. power	600 MW _e
		<u>Inner rings</u>	<u>Outer rings</u>
Major radius (m)		8.0	14.4
Stored energy (GJ)		5.3	11
Force on ring (MN)		-18.6	+28.0 (compr.)
Mass of ring (tonnes)		1200	2160

This reactor design also included two possible power cycles, a steam cycle at 540°C and a helium gas-turbine Brayton cycle at 870°C, both providing = 44% efficiency with present technology. The problems of impurity control, refueling, and ash removal remain to be solved, as with mainline approaches. However, ash removal is a particularly critical problem in advanced-fuel reactors because the fraction of available β used to confine the reaction products decreases the already low value of fuel density.

RING STABILITY

The critical problem of mechanically stabilizing the floating rings has been examined by several independent workers, and the situation is summarized in Ref. 2. Since the rings carry current in the same direction, they attract one another and must be separated by large forces provided by currents in the walls or external coils. Each ring has five degrees of freedom: slide in two directions, tilt around two axes, and vertical displacement. Stability of pulsed multi-ring systems has been demonstrated by the Wisconsin octupole and the UCLA dodecapole. The long-term stability of superconducting rings, however, has been achieved only with active feedback and only on single-ring systems. Reliance on passive stabilization alone would obviously be desirable in a reactor. A study by the TRW group² shows that the use of shorted turns in the shape shown in Fig. 11 would stabilize one motion at a time. The simultaneous stabilization of many rings interacting with one another using passive conductors well outside the plasma has not yet been shown possible, but it is believed that at worst only a small amount of active feedback control needs to be added to a passive system. L. Heflinger⁷ has invented a clever device to test stabilizing windings. A small model is constructed, and the inductance of a given hoop is used as part of the resonant circuit of an oscillator. Motion of the hoop changes the frequency of the oscillator up or down depending on how the inductance is changed. The existence of a stable, maximum inductance state is then easily discovered.

OTHER STUDIES

A step-by-step program to investigate the ultimate feasibility of multipole reactors has been proposed². The elements are a) a large octupole, using cryogenic but not superconducting Al rings, for testing the physics scaling of confinement time and beta limits up to kilovolt temperatures, using neutral beam heating; b) a technology validation test of a large superconducting Nb₃Sn ring; c) a tabletop superconducting experiment to test

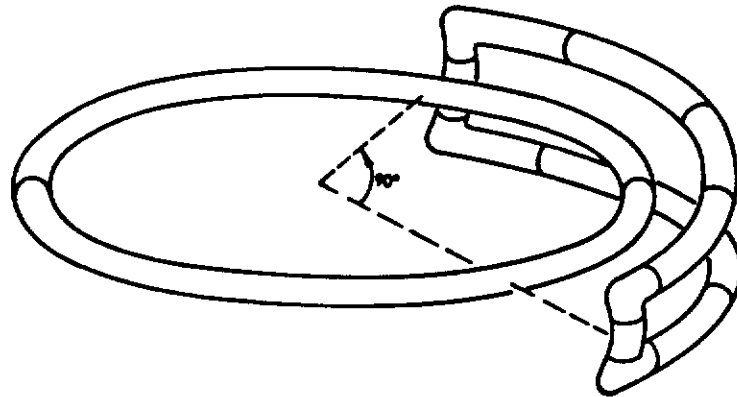


Fig. 11. A passive quadrant stabilizer for a floating ring.

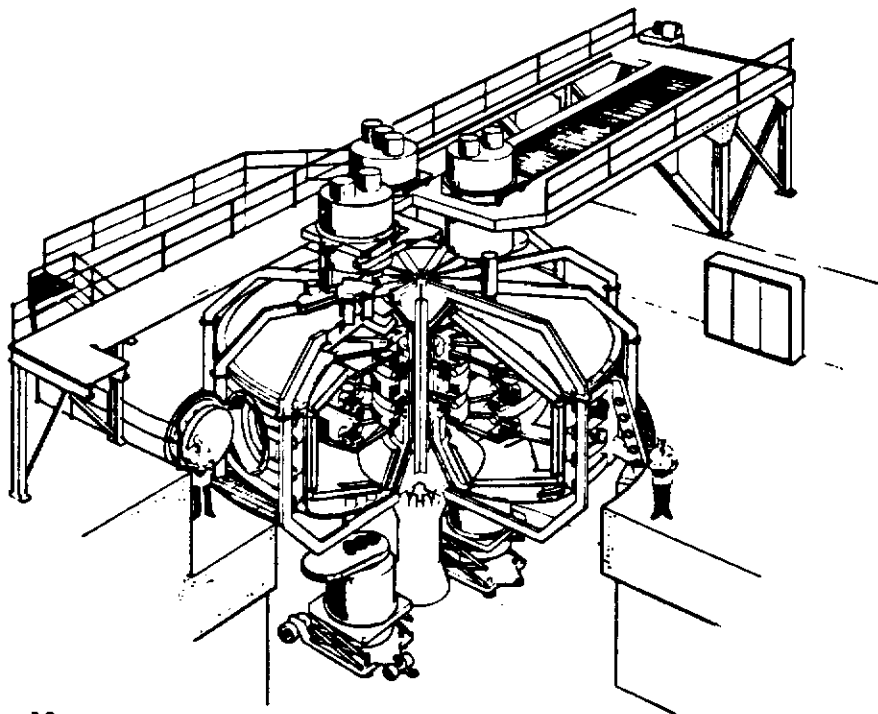


Fig. 12. A cryogenic octupole designed for test of scaling laws.

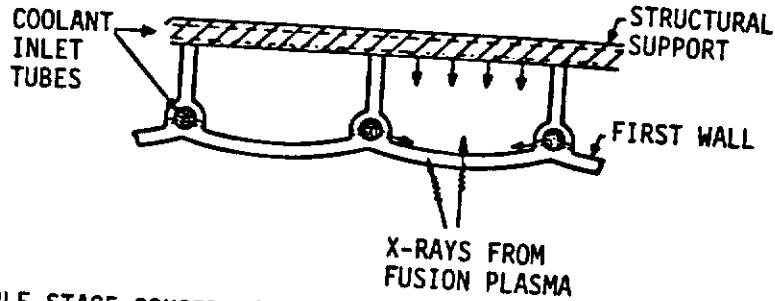
stabilization of octupole rings; and d) a large proof-of-principle experiment using these technological developments. The first of these devices has been designed in some detail; a sketch of it is shown in Fig. 12. Though multipole-surmac reactors are less well developed in concept than DT reactors in tokamak or tandem mirror configurations, it appears that an orderly progression of physics and engineering test devices is possible to examine the feasibility of the concept once the basic question of nuclear reaction rates is settled.

FUTURE POSSIBILITIES

The multipole-surmac advanced-fuel reactor concept provides an opportunity for generating new, daring ideas. One of these, the idea of building a liquid He cryostat into each floating ring, has already been mentioned. Another unconventional scheme, also not developed beyond the initial thought stage, has been proposed by A. Hertzberg⁸. Here, use is made of the fact that the x-ray output of a neutronless fuel cycle constitutes a high-grade form of energy. The x-rays pass through a thin, low-Z first wall (Fig. 13) and are absorbed by a high-Z gas coolant. Alternatively, tungsten glow-plates can be used to absorb the x-rays and heat the coolant gas by contact. A temperature gradient across the gas allows the outlet temperature to be higher than the wall temperature, thus increasing the thermal efficiency above the normal 40% level. The hot gas is then expanded in a rotating acoustic wave convertor (Fig. 14) to drive a high-pressure helium turbine. It is estimated that efficiencies of 50-65% may be possible.

A third idea, well within the realm of possibility, has been proposed by Dawson⁹ for heating plasmas by means of beams of partially ionized light ions. For instance, 100 A of 10-MeV Li^+ ions would give 1 GW of heating power. Though accelerators of this voltage-current range do not exist, they are not far beyond present capabilities. The light ions would be fully stripped by the plasma and become trapped. Good injection orbits for a tokamak are somewhat difficult to achieve, since it is best to inject from the inside of the torus, where there is little space; but injection into a multipole-surmac would be quite simple. Fig. 15a shows the dimensions of a conceptual p-B11 dodecapole surmac reactor for which some numerical computations have been made¹⁰. Fig. 15b shows the path of an injected 10-MeV B^{11} ion before it is ionized to Z=2. Figs. 15c and 15d show the paths of the ion while in the Z=3 and Z=4 states. It is seen that the ions are easily trapped and trace out the bridge regions clearly. Ions in this energy range are indistinguishable from the promoted tail of the distribution function and can be treated in the same manner. Plasma heating is probably not the most difficult problem in an advanced-fuel multipole.

SINGLE STAGE CONCEPTS(High Z coolant, Low Z wall)



MULTIPLE STAGE CONCEPTS(High Z glow, Low Z wall)

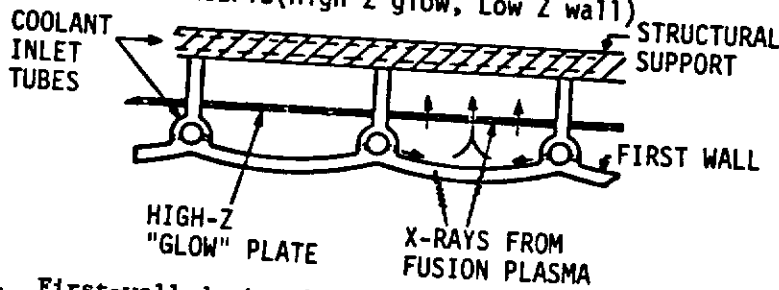
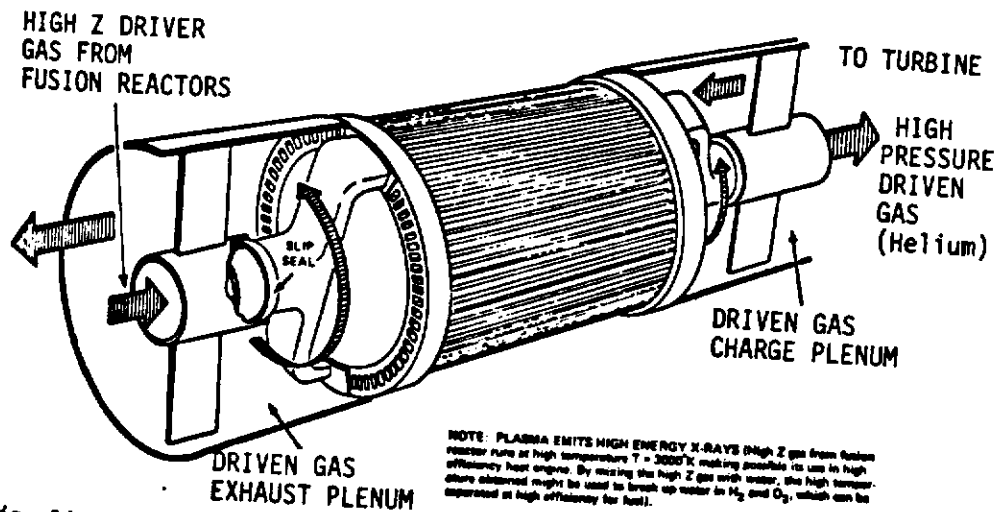


Fig. 13. First-wall design for absorption of x-ray energy output.



NOTE: PLASMA EMITS HIGH ENERGY X-RAYS (High Z gas from fusion reactor runs at high temperature $T = 3000^{\circ}\text{K}$, making possible its use in high efficiency heat engine. By mixing the high Z gas with water, the high temperature obtained might be used to break up water in H_2 and O_2 , which can be separated at high efficiency for fuel).

Fig. 14. High-efficiency heat engine employing high-Z driver gas.

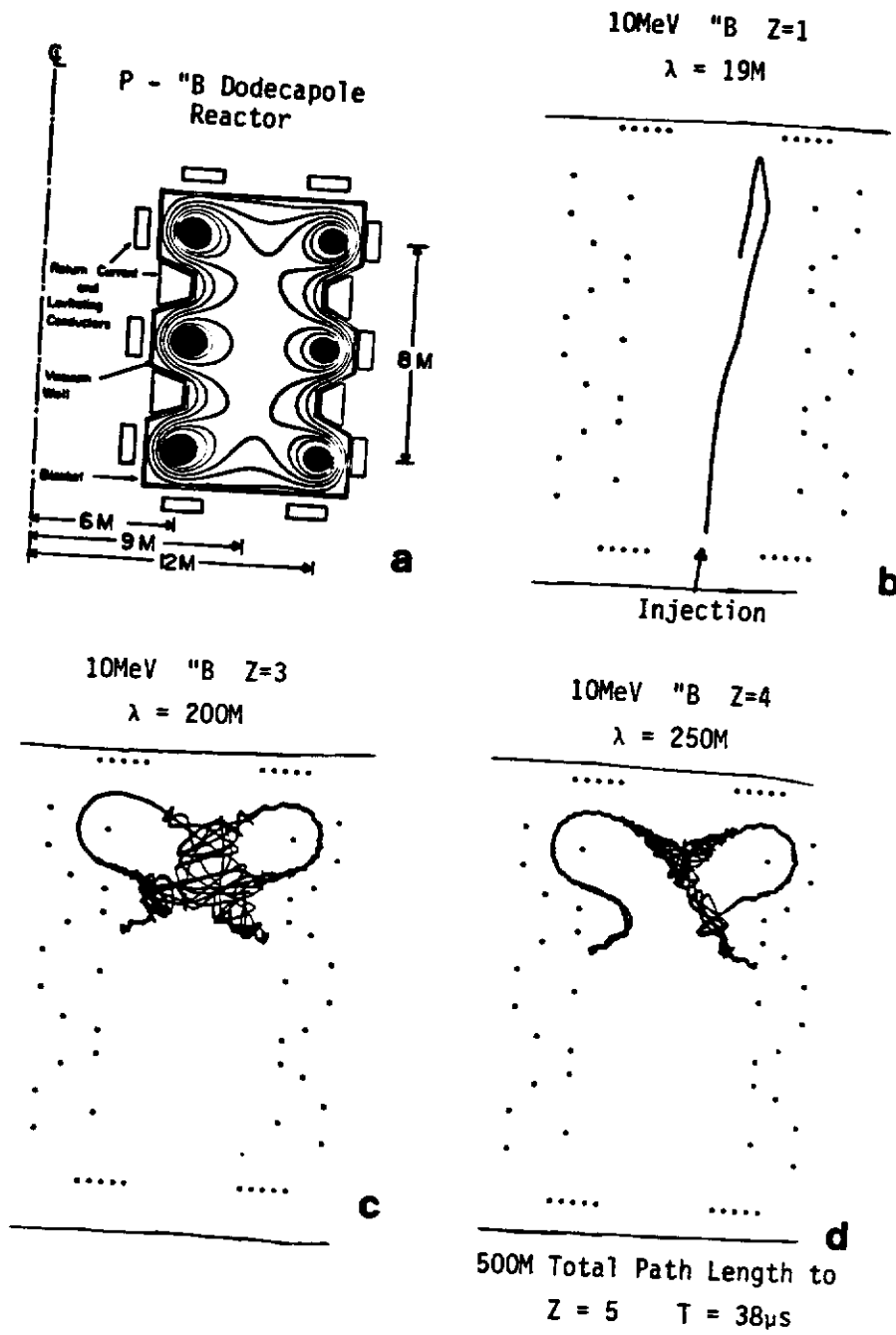


Fig. 15. Ion beam heating of a surmac reactor (a). The path of a 10-MeV B^+ injected ion is shown in (b)-(d) as it goes through the Z=1 to Z=4 ionization states.

ACKNOWLEDGMENTS

We have had the benefit of conversations with R. W. Conn, G. Shuy, S. Grosz, L. Heflinger, R. Schumacher, and J. M. Dawson. We are particularly grateful to R. W. Conn and his colleagues for releasing the results of their computations for this review in advance of their publication.

REFERENCES

1. R. W. Conn et al., Alternate fusion fuel cycle research, Plasma Physics and Controlled Nuclear Fusion Research 1980, paper IAEA-CN-38/V-5, IAEA, Vienna (1981, to be published).
2. TRW Group, EPRI Project Report RP-1190, Electric Power Research Institute, Palo Alto, California (1981, to be published).
3. R. W. Conn and G. Shuy, Univ. of Wisconsin Report UWFD-262 (1978).
4. G. W. Shuy and R. W. Conn, Physics phenomena in the analysis of advanced fusion fuel cycles, UCLA Report PPG-522 (1980).
5. G. W. Shuy, Thesis, University of Wisconsin (1980).
6. S. Grosz, UCLA, private communication.
7. L. Heflinger, TRW, private communication and Ref. 2.
8. A. Hertzberg, in The EPRI Asilomar Papers, EPRI Special Report ER-378-SR, Electric Power Research Institute, Palo Alto, California (1977).
9. J. M. Dawson, private communication.
10. R. W. Schumacher and G. Hockney, private communication.